

REPORT DOCUMENTATION PAGE				Form Approved OMB NO. 0704-0188	
<p>The public reporting burden for this collection of information is estimated to average 1 hour per response, including the time for reviewing instructions, searching existing data sources, gathering and maintaining the data needed, and completing and reviewing the collection of information. Send comments regarding this burden estimate or any other aspect of this collection of information, including suggestions for reducing this burden, to Washington Headquarters Services, Directorate for Information Operations and Reports, 1215 Jefferson Davis Highway, Suite 1204, Arlington VA, 22202-4302. Respondents should be aware that notwithstanding any other provision of law, no person shall be subject to any penalty for failing to comply with a collection of information if it does not display a currently valid OMB control number.</p> <p>PLEASE DO NOT RETURN YOUR FORM TO THE ABOVE ADDRESS.</p>					
1. REPORT DATE (DD-MM-YYYY)		2. REPORT TYPE New Reprint		3. DATES COVERED (From - To) -	
4. TITLE AND SUBTITLE Multiple Aerosol Unmixing by the Split Bregman Algorithm				5a. CONTRACT NUMBER W911NF-09-1-0383	
				5b. GRANT NUMBER	
				5c. PROGRAM ELEMENT NUMBER 611103	
6. AUTHORS Russell E. Warren, Stanley J. Osher, Richard G. Vanderbeek				5d. PROJECT NUMBER	
				5e. TASK NUMBER	
				5f. WORK UNIT NUMBER	
7. PERFORMING ORGANIZATION NAMES AND ADDRESSES William Marsh Rice University Office of Sponsored Research 6100 Main St., MS-16 Houston, TX 77005 -1827				8. PERFORMING ORGANIZATION REPORT NUMBER	
9. SPONSORING/MONITORING AGENCY NAME(S) AND ADDRESS(ES) U.S. Army Research Office P.O. Box 12211 Research Triangle Park, NC 27709-2211				10. SPONSOR/MONITOR'S ACRONYM(S) ARO	
				11. SPONSOR/MONITOR'S REPORT NUMBER(S) 56177-CS-MUR.177	
12. DISTRIBUTION AVAILABILITY STATEMENT Approved for public release; distribution is unlimited.					
13. SUPPLEMENTARY NOTES The views, opinions and/or findings contained in this report are those of the author(s) and should not be construed as an official Department of the Army position, policy or decision, unless so designated by other documentation.					
14. ABSTRACT For more than a decade, the U.S. government has been developing laser-based sensors for detecting, locating, and classifying aerosols in the atmosphere at safe standoff ranges. The motivation for this work is the need to discriminate aerosols of biological origin from interferent materials such as smoke and					
15. SUBJECT TERMS Aerosols, lidar, L1-regularization, parameter estimation, remote sensing					
16. SECURITY CLASSIFICATION OF:			17. LIMITATION OF ABSTRACT UU	15. NUMBER OF PAGES	19a. NAME OF RESPONSIBLE PERSON Richard Baraniuk
a. REPORT UU	b. ABSTRACT UU	c. THIS PAGE UU			19b. TELEPHONE NUMBER 713-348-5132

Report Title

Multiple Aerosol Unmixing by the Split Bregman Algorithm

ABSTRACT

For more than a decade, the U.S. government has been developing laser-based sensors for detecting, locating, and classifying aerosols in the atmosphere at safe standoff ranges. The motivation for this work is the need to discriminate aerosols of biological origin from interferent materials such as smoke and dust using the backscatter from multiple wavelengths in the long wave infrared (LWIR) spectral region. Through previous work, algorithms have been developed for estimating the aerosol spectral dependence and concentration range dependence from these data. The range dependence is required for locating and tracking the aerosol plumes, and the backscatter spectral dependence is used for discrimination by a support vector machine classifier. Substantial progress has been made in these algorithms for the case of a single aerosol present in the lidar line-of-sight (LOS). Often, however, mixtures of aerosols are present along the same LOS overlapped in range and time. Analysis of these mixtures of aerosols presents a difficult inverse problem that cannot be successfully treated by the methods used for single aerosols. Fortunately, recent advances have been made in the analysis of inverse problems using shrinkage-based L1-regularization techniques. Of the several L1-regularization methods currently known, the split Bregman algorithm is straightforward to implement, converges rapidly, and is applicable to a broad range of inverse problems including our aerosol unmixing. In this paper, we show how the split Bregman algorithm can successfully resolve LWIR lidar data containing mixtures of bioaerosol simulants and interferents into their separate components. The individual components then can be classified as bio- or nonbioaerosol by our SVM classifier. We illustrate the approach through data collected in field tests over the past several years using the U.S. Army FAL sensor in testing at Dugway Proving Ground, UT.

REPORT DOCUMENTATION PAGE (SF298)
(Continuation Sheet)

Continuation for Block 13

ARO Report Number 56177.177-CS-MUR
Multiple Aerosol Unmixing by the Split Bregman ...

Block 13: Supplementary Note

© 2012 . Published in IEEE Transactions on Geoscience and Remote Sensing, Vol. Ed. 0 50, (9) (2012), (, (9). DoD Components reserve a royalty-free, nonexclusive and irrevocable right to reproduce, publish, or otherwise use the work for Federal purposes, and to authorize others to do so (DODGARS §32.36). The views, opinions and/or findings contained in this report are those of the author(s) and should not be construed as an official Department of the Army position, policy or decision, unless so designated by other documentation.

Approved for public release; distribution is unlimited.

Multiple Aerosol Unmixing by the Split Bregman Algorithm

Russell E. Warren, *Member, IEEE*, Stanley J. Osher, and Richard G. Vanderbeek

Abstract—For more than a decade, the U.S. government has been developing laser-based sensors for detecting, locating, and classifying aerosols in the atmosphere at safe standoff ranges. The motivation for this work is the need to discriminate aerosols of biological origin from interferent materials such as smoke and dust using the backscatter from multiple wavelengths in the long wave infrared (LWIR) spectral region. Through previous work, algorithms have been developed for estimating the aerosol spectral dependence and concentration range dependence from these data. The range dependence is required for locating and tracking the aerosol plumes, and the backscatter spectral dependence is used for discrimination by a support vector machine classifier. Substantial progress has been made in these algorithms for the case of a single aerosol present in the lidar line-of-sight (LOS). Often, however, mixtures of aerosols are present along the same LOS overlapped in range and time. Analysis of these mixtures of aerosols presents a difficult inverse problem that cannot be successfully treated by the methods used for single aerosols. Fortunately, recent advances have been made in the analysis of inverse problems using shrinkage-based L_1 -regularization techniques. Of the several L_1 -regularization methods currently known, the split Bregman algorithm is straightforward to implement, converges rapidly, and is applicable to a broad range of inverse problems including our aerosol unmixing. In this paper, we show how the split Bregman algorithm can successfully resolve LWIR lidar data containing mixtures of bioaerosol simulants and interferents into their separate components. The individual components then can be classified as bio- or nonbioaerosol by our SVM classifier. We illustrate the approach through data collected in field tests over the past several years using the U.S. Army FAL sensor in testing at Dugway Proving Ground, UT.

Index Terms—Aerosols, lidar, L_1 -regularization, parameter estimation, remote sensing.

I. INTRODUCTION

THIS WORK describes a generalization of previous research [1] on developing efficient algorithms for estimating the parameters of optically thin aerosols in the atmosphere using data from rapidly tuned multiple-wavelength long wave infrared (LWIR) lidar [2]. The motivation for this work remains the same: the need for detecting, locating, track-

ing, and discriminating atmospheric aerosols at safe standoff ranges using time-series data collected at a discrete set of CO_2 laser wavelengths. Our earlier work considered a single aerosol material, producing a backscatter enhancement over that from the natural atmosphere. The goals were to detect and track the aerosol by means of estimates of the range dependence of the concentration, and to discriminate potentially harmful aerosols—particularly those of biological origin—from interferents such as smoke and dust by means of the spectral dependence of the backscatter. State-of-the-art support vector machine (SVM) classifiers have been developed for this discrimination.

Often, however, mixtures of aerosols are present along the same lidar line-of-sight (LOS), overlapped in range and time. For example, it is quite possible to have a biological or chemical agent release from a munition accompanied by dust and other byproducts of the explosive release. Those extra materials can distort the spectral dependence of the threat material and degrade the ability of the sensor to correctly identify the threat. The analysis of aerosol mixtures presents a difficult inverse problem that cannot be successfully treated by the methods used previously for single materials.

Fortunately, recent advances have been made in the analysis of inverse problems using shrinkage-based L_1 -regularization techniques. We focus here on the split Bregman algorithm [3] because it is straightforward to implement, converges rapidly, and is applicable to a broad range of inverse problems including our aerosol unmixing. In this paper, we show how the split Bregman algorithm can successfully resolve LWIR lidar data containing mixtures of bioaerosol simulants and interferents into their separate components. The individual components then can be classified as bio- or nonbioaerosol by our SVM classifier.

The use of Bregman iteration to solve difficult L_1 -estimation problems efficiently was described by Yin *et al.* [4]. In that paper, they showed the equivalence of Bregman iteration to the augmented Lagrangian method for the minimization of convex functions with linear constraints. In a subsequent paper, Goldstein and Osher [3] showed that Bregman iteration could be efficiently implemented by splitting the original combination of L_1 and L_2 optimizations over a single variable into two separate minimizations: one over a differentiable quadratic component, and a second over a nondifferentiable L_1 -norm component with an objective function that could be solved in closed form by shrinkage. This is the origin of the term “split Bregman.” Subsequently, [5], [6], it was recognized that their splitting algorithm could be interpreted from a Lagrangian and

Manuscript received June 3, 2011; revised October 12, 2011; accepted December 11, 2011. Date of publication February 3, 2012; date of current version August 22, 2012. This work was supported in part by the U.S. Army RDECOM Contract W911SR-10-C-0067 and in part by National Science Foundation under Grant DMS0914561.

R. E. Warren is with the EO-Stat Inc., Chapel Hill, NC 27517 USA (e-mail: eostatinc@aol.com).

S. J. Osher is with the University of California, Los Angeles, CA 90095 USA (e-mail: sjo@math.ucla.edu).

R. G. Vanderbeek is with the U. S. Army Edgewood Chemical Biological Center, Aberdeen, MD 21010 USA (e-mail: richard.vanderbeek@us.army.mil).

Digital Object Identifier 10.1109/TGRS.2011.2180913

penalty standpoint (augmented Lagrangian) analogous to that described in [4]. It is this augmented Lagrangian interpretation of split Bregman that we follow here. For a comprehensive analysis of the interrelations between Bregman iteration, augmented Lagrangians, split Bregman, and other techniques, see the review by Esser [7].

The spectral unmixing problem is of course well known in the context of hyperspectral (HS) imagery, and hundreds of papers have been devoted to algorithms for performing it [8]. In the simplest case when multiple scattering from neighboring topographical features can be ignored, the HS unmixing problem can be solved by least squares methods if the endmember spectra are known. The latter can be identified by principal components analysis using training data. Our problem is roughly similar to HS, but quite distinct. First, whereas HS images have typically hundreds of spectral lines available and of the order of 10^4 pixels in a fixed image, our FAL data have only 19 CO₂ wavelengths and at most hundreds of time steps and range cells in a dynamically changing environment. Most importantly, we have no well-defined prior spectra on which to base the analysis; we must estimate both the spectra and concentration (the analog of abundance in HS) from the same data. For these reasons, the lidar unmixing problem is substantially more difficult than HS, and we are not aware of prior publications in this area.

In our treatment of single aerosol estimation, we gave a rather detailed discussion of the lidar measurement and preprocessing needed to remove the effects of the natural atmosphere and to deconvolve the long CO₂ transmitter pulse waveforms. Those discussions pertain here without any modification. However, to make the aerosol unmixing discussion intelligible to a broader readership, in Section II, we summarize the main ideas underlying rapidly tuned multiwavelength backscatter lidar for aerosol standoff sensing. Following that, we concentrate on the problem of parameter estimation for multiple aerosols by use of the split Bregman method. Accordingly, Section III provides a brief summary of the advantages of L_1 -regularization over the more traditional L_2 method, and more particularly, how this newer, more robust method can be implemented efficiently through split Bregman. Section IV describes how the multi-aerosol estimation is formulated as a dual application of the basic split Bregman algorithm. In Section V, we give some examples of processing aerosol mixture data from both simulated and actual release data collected by the U.S. Army FAL sensor during testing at Dugway Proving Ground, UT. Section VI summarizes and concludes.

II. MULTIWAVELENGTH LIDAR FOR AEROSOL SENSING

In this section, we review the main ideas behind aerosol standoff sensing using rapidly tuned multiwavelength elastic backscatter lidar operating in the LWIR spectral region. A more comprehensive treatment is given in [1].

The measurement configuration is as follows. At each time step a set of M -wavelength-pulses separated in time by 5 ms is transmitted and partially backscattered to the lidar receiver. The transmitter cycles through the wavelengths in each set in a prescribed pattern chosen either to emphasize certain spectral

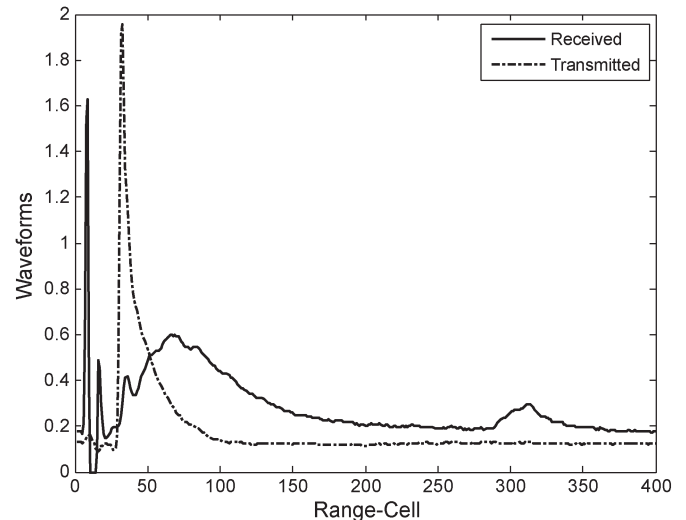


Fig. 1. Transmitted and received lidar waveforms at a single time step and wavelength.

features in the 9–11 μm spectral region accessible to the lidar, or to provide a reasonably uniform wavelength sampling of that entire range. Each transmitter pulse waveform is continuously scattered by aerosols along the lidar LOS. The backscattered temporal waveforms are photodetected, electronically filtered, digitized, and stored at each wavelength within the transmitted set at each time step.

The goals of the processing are to use the digitized transmitted and received backscatter array data to 1) decide if significant aerosol is present; 2) provide estimates of the range and size of the aerosol cloud; and 3) produce estimates of the backscatter spectral dependence for use by an aerosol classifier. Because of the time-series nature of the data collection, these functions must be performed sequentially using the current and past data together with background data samples (data not containing release aerosols) collected at the deployment site. These background data samples are essential for normalizing the data that are to be analyzed for the presence of target aerosols.

Prior to the main processing algorithms used to estimate the aerosol backscatter spectral dependence and concentration range dependence, there is a preprocessing step to estimate and remove: 1) nonzero baselines in the transmitted and received waveforms; 2) the backscatter from the ambient atmosphere; and 3) the distortion caused by the transmitted pulse waveforms. The latter effect is the result of a combination of laser firing delay, long CO₂ pulse duration, and random shape effects in the tail of the pulse. A deconvolution filter based on the Wiener-Helstrom method was used for the pulse deconvolution. Fig. 1 shows these effects by plotting the transmitted and received waveforms versus range cell from time step 200 at one (10R38) of the 19 transmitted CO₂ wavelengths of the mixture release TD4065 from the U.S. Army FAL sensor. The natural atmospheric aerosol backscatter is present up to about range cell 250. This structure must be removed prior to the backscatter and concentration estimation. The smaller structure around range cell 320 is the target aerosol, the bacillus BG in this case.

Our model for the aerosol backscatter at the lidar receiver following baseline subtraction and ambient aerosol backscatter removal is then

$$P_{ijk} = \sum_{k'=1}^k G_{ijk'} T_{ij,k-k'+1} + \varepsilon_{ijk} \quad (1)$$

where P_{ijk} is the received lidar waveform at time step i , wavelength j , $1 \leq j \leq M$, and digitized range cell k , $1 \leq k \leq N$, T_{ijk} is the corresponding transmitted lidar pulse waveform, and G_{ijk} is the lidar response for a delta-pulse transmitter, and ε_{ijk} is an additive noise term taken to be zero mean, independent, and identically distributed (i.i.d.) for each wavelength. We model G as

$$G_{ijk} = g_j \sum_{l=1}^L \rho_{ijl} C_{lik} \quad (2)$$

in terms of the aerosol backscatter coefficient ρ_{ijl} for material l , $1 \leq l \leq L$, C_{lik} is the aerosol range-dependent concentration, and g_j is a generally wavelength-dependent lidar efficiency factor. The wavelength dependence reflects that of the detector and optics. In the absence of knowledge of g , we set it to unity. The pulse-deconvolution filter provides us with an estimate of G

$$\hat{G}_{ijk} = G_{ijk} + n_{ijk} \quad (3)$$

where n_{ijk} is an additive noise from the filtered input noise ε , again assumed to be zero mean and i.i.d. The wavelength dependence of the backscatter coefficients ρ is a composite result of the wavelength dependence of the complex refractive index of the aerosol materials and diffraction effects from the particle size distributions of each of the L aerosols.

Our goal in the data processing is to estimate ρ and C as functions of time, wavelength (ρ) or range (C), and material. Because of their appearance in G as the sum of products, we cannot expect to obtain estimates having the correct units without further information and must settle for relative estimates. For simplicity, we have required that ρ for each time and material be unit vectors in wavelength lying in the positive orthant

$$\sum_{j=1}^M \rho_{ijl}^2 = 1, \quad \rho_{ijl} \geq 0 \quad (4)$$

and $C_{lik} \geq 0$.

III. L_1 -REGULARIZATION OF INVERSE PROBLEMS BY THE SPLIT BREGMAN METHOD

It is well known that inverse problems (such as the retrieval of signals observed after some smoothing operation such as blurring) are ill-posed in the sense of Hadamard: small changes in the data due to noise, for example, can have large effects on the solution. Otherwise stated, many different solutions are compatible with the same data. Since most of these “solutions” are wildly oscillatory, and therefore not physically meaningful, some sort of regularization is required to produce useful results. Historically, L_2 -regularization has been used in the context of

least-squares estimation since it is easy to implement through ridge regression. Although stabilizing the solution, ridge regression tends to be unselective in the features it suppresses and can lead to severely biased results.

As noted above, more recent alternatives to L_2 -regularization have replaced the quadratic regularization term in the objective function with an L_1 -norm regularizing term. This has the effect of selectively removing features in the estimate that produce the large fluctuations associated with direct inversion without regularization. This selectivity gives L_1 estimates a sparse representation in an appropriate basis set. The downside of L_1 -regularization has been the loss of differentiability of the objective function making implementation more difficult than L_2 .

As noted above, the new class of shrinkage-based inversion methods such as split Bregman largely overcomes the computational limitations of L_1 -regularization. To illustrate the advantages of L_1 over L_2 , we compare them on a simple 1-D simulated example. Our objective is to minimize the functionals $J_1(u)$ and $J_2(u)$

$$\begin{aligned} \hat{u}_{1,2} &= \arg \min_u J_{1,2}(u), \\ J_1(u) &= \frac{1}{2} \|Ku - f\|_2^2 + \lambda \|u\|_1, \\ J_2(u) &= \frac{1}{2} \|Ku - f\|_2^2 + \frac{\mu}{2} \|u\|_2^2 \end{aligned} \quad (5)$$

where $J_{1,2}$ are the sum of a quadratic term quantifying the fidelity of the linear model Ku to the data f , and the second terms are regularizers using the L_1 and L_2 norms, respectively

$$\|u\|_1 \equiv \sum_k |u_k|, \quad \|u\|_2 \equiv \left[\sum_k |u_k|^2 \right]^{1/2}. \quad (6)$$

We assume the model operator K and the data to be known. The scalar coefficients λ and μ are set heuristically to balance the conflicting needs for fitting the model and solution smoothness.

For concreteness, we modeled u as the sum of two narrow Gaussian functions given by

$$u(x) = \exp[-(x+0.1)^2/0.001] + \exp[-(x-0.1)^2/0.001] \quad (7)$$

and shown in Fig. 2 sampled uniformly over 1000 points between -2 and 2 . The data f were created by blurring u with a Toeplitz matrix

$$K_{nm} = \frac{1}{50} r^{|n-m|} \quad (8)$$

with $r = 0.99$, and adding zero-mean independently distributed (pseudo-)random normal noise with standard error $\sigma = 0.004$

$$\begin{aligned} f_n &= \sum_m K_{nm} u_m + q_n, \\ q_n &\sim N(0, \sigma^2). \end{aligned} \quad (9)$$

The simulated data are shown in Fig. 2 together with the L_2 regression estimate at the value $\mu = 0.015$, and the L_1 estimate computed by the split Bregman method defined below also using $\lambda = 0.015$. We note the L_2 estimate is unable to resolve

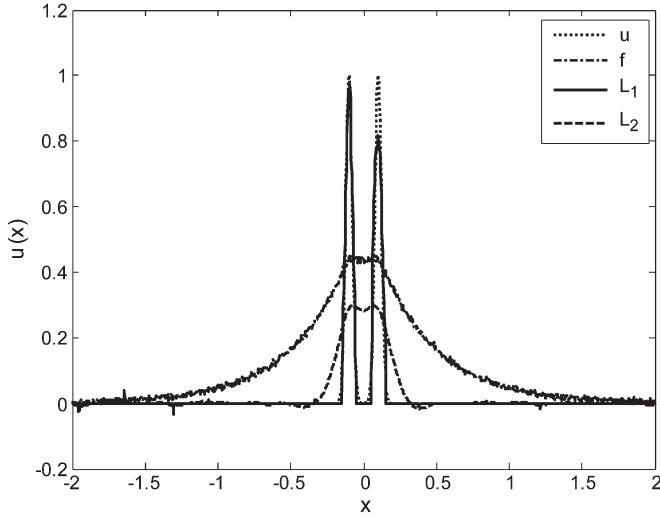


Fig. 2. Data and estimates from the blurred narrow Gaussian example.

the peaks, whereas the L_1 estimate gives a clean separation of the two components.

The objective function J_1 is nonsmooth because of the L_1 -norm regularization term. This makes the optimization over u difficult by the usual calculus-based methods. The basic idea of split Bregman is to introduce additional variables into the J_1 objective function that will allow a convenient separation of the minimizations over the quadratic (smooth) data term

$$H(u) = \frac{1}{2} \|Ku - f\|_2^2 \quad (10)$$

and the nonsmooth regularization term $\|u\|_1$. This is done in two steps. First, the unconstrained problem $\arg \min_u H(u) + \|u\|_1$ is replaced by the equivalent constrained problem

$$\arg \min_u H(u) + \mu \|d\|_1 \text{ such that } u = d. \quad (11)$$

Second, the constraint $u = d$ is enforced by adding a Lagrange multiplier term and an additional quadratic penalty term to get the Lagrangian

$$L(u, d, b) = H(u) + \mu \|d\|_1 + \lambda \langle b, u - d \rangle + \frac{\lambda}{2} \|u - d\|_2^2 \quad (12)$$

where b is the Lagrange multiplier vector, $\langle a, b \rangle$ denotes the inner product of vectors a and b , and μ and λ are positive regularization parameters. In this formulation, L assumes the form of an augmented Lagrangian [4], [5] to be minimized for u and d , and maximized for the dual variable b . In the Appendix, the derivation of this saddle point optimization is sketched. The resulting algorithm is given as Algorithm 1. The function $S_\lambda(x)$ appearing in Algorithm 1 is the shrinkage operator that plays a key role in the success of the method by promoting sparseness in the solution through shrinking input values toward zero. S is defined as

$$S_\lambda(x) \equiv \begin{cases} x - \lambda, & x > \lambda \\ 0, & -\lambda \leq x \leq \lambda \\ x + \lambda, & x < -\lambda \end{cases}. \quad (13)$$

Algorithm 1. Split Bregman algorithm.

Initialization: $d^0 = b^0 = 0, k = 0, \|\Delta u\|_2 = 1$
 while $\|\Delta u\|_2 > \varepsilon$,
 $u^{k+1} = (K^T K + \lambda I)^{-1} (K^T f + \lambda(d^k - b^k))$,
 $d^{k+1} = S_{\mu/\lambda}(u^{k+1} + b^k)$,
 $b^{k+1} = b^k + u^{k+1} - d^{k+1}$,
 $\Delta u = u^{k+1} - u^k$,
 $k \rightarrow k + 1$,
 end

IV. MULTI-AEROSOL SPLIT BREGMAN ALGORITHM

In this section, we generalize the basic split Bregman method described in Section III to treat the aerosol unmixing problem for multiple aerosols within a single lidar LOS. Our starting point is the $M \times N$ matrix $G = \{G_{jk}\}$ given by (2) (suppressing the time-index i) that represents the range-resolved lidar data at a single time step after the preprocessing to remove the natural aerosol backscatter and transmitter pulse effects as summarized in Section II.

Our goal is to resolve G into L aerosol components using a generalization of the L_1 -regularized split Bregman method. The problem then is to solve

$$\min_{\|\rho\|=1, \rho \geq 0, C \geq 0} \mu_\rho |\rho|_1 + \mu_C |C|_1 + \frac{1}{2} \|G - \rho C\|_F^2 \quad (14)$$

where $|x|_1$ denotes the L_1 norm $\sum_k |x_k|$, and $\|\cdot\|_F$ indicates the matrix Frobenius norm

$$\|G - \rho C\|_F^2 \equiv \sum_{j,k} \left[G_{jk} - \sum_{l=1}^L \rho_{jl} C_{lk} \right]^2. \quad (15)$$

Due to the coupling between ρ and C through the term $\|G - \rho C\|_F^2$ we do not have a convex problem. Our approach is to iteratively solve for ρ assuming C and vice versa through a series of subproblems each of which is convex and solvable by the split Bregman/augmented Lagrangian method. Although the method has worked well on simulated and actual data, we cannot claim optimality for the overall solution.

To split the problem into a series of manageable steps, we introduce the auxiliary variables r and c for ρ and C , and formulate the augmented Lagrangian problem

$$\min_{\rho, C} \min_{\|r\|=1, r \geq 0, c \geq 0} \mu_\rho |r|_1 + \mu_C |c|_1 + \frac{1}{2} \|G - \rho C\|_F^2 + \frac{\lambda_r}{2} \|r - \rho - b_r\|_F^2 + \frac{\lambda_c}{2} \|c - C - b_c\|_F^2. \quad (16)$$

The parameters $\mu_\rho, \lambda_r > 0$ and $\mu_C, \lambda_c > 0$ control the balance between fitting errors and parameter smoothness, and are set heuristically using a combination of simulated and test data. The auxiliary parameters r and c serve two functions: they enforce the constraints and split the L_1 and L_2 minimizations. The parameters b_r and b_c are the Lagrange dual variables (subgradients) that enforce the constraints $\rho = r$ and $C = c$.

Because the auxiliary variables now carry the positivity and unit norm constraints, the subproblems for ρ and C are unconstrained, and can be solved by differentiation. The resulting updates are

$$\begin{aligned} C &= (\rho^T \rho + \lambda_c I)^{-1} (\rho^T G + \lambda_c (c - b_c)) \\ \rho &= (C C^T + \lambda_r I)^{-1} (C G^T + \lambda_r (r - b_r)). \end{aligned} \quad (17)$$

The constrained subproblem for c becomes

$$\min_{c \geq 0} \mu_C |c|_1 + \frac{\lambda_c}{2} \|c - C - b_c\|_F^2 \quad (18)$$

having the solution

$$c = \max(C + b_c - \mu_C / \lambda_c, 0) \equiv (C + b_c - \mu_C / \lambda_c)^+. \quad (19)$$

The subproblem for r is slightly more complicated since we require both $\|r\| = 1$ and $r \geq 0$. We have to solve

$$\min_{\|r\|=1, r \geq 0} \mu_\rho |r|_1 + \frac{\lambda_r}{2} \|r - \rho - b_r\|_F^2. \quad (20)$$

The constrained solution for r is

$$r = \frac{(\rho + b_r - \mu_\rho / \lambda_r)^+}{\|(\rho + b_r - \mu_\rho / \lambda_r)^+\|}. \quad (21)$$

We have verified that this solution does indeed satisfy the KKT (Karush–Kuhn–Tucker) optimality conditions [9]. Finally, the subgradients at each iteration are updated as

$$\begin{aligned} b_r &\rightarrow b_r + \rho - r, \\ b_c &\rightarrow b_c + C - c. \end{aligned} \quad (22)$$

Algorithm 2 gives the resulting unmixing algorithm. The recursions in Algorithm 2 are initialized by prior estimates ρ_{prior} of the backscatter, if available, or randomly. Typically, 10–30 iterations are enough to give good results.

Algorithm 2. Split Bregman algorithm for multi-aerosol unmixing.

```

Initialize  $\rho^0$  through prior estimate  $\rho_{\text{prior}}$  or randomly.
 $D\rho = 1, \rho_{\text{old}} = 0$ 
while  $D\rho > \varepsilon$ 
   $r^0 = c^0 = b_r^0 = b_c^0 = 0, n = 0, C^0 = 0, \|\Delta C\|_F = 1$ 
  while  $\|\Delta C\|_F > \varepsilon$ 
     $C^{n+1} = (\rho^{nT} \rho^n + \lambda_c I)^{-1} (\rho^{nT} G + \lambda_c (c^n - b_c^n))$ ,
     $c^{n+1} = (C^{n+1} + b_c^n - \mu_c / \lambda_c)^+$ ,
     $b_c^{n+1} = b_c^n + C^{n+1} - c^{n+1}$ ,
     $\Delta C = C^{n+1} - C^n$ ,
     $n \rightarrow n + 1$ ,
  end
   $\hat{C} = C^{n+1}, \|\Delta \rho\|_F = 1, n = 0$ 
  while  $\|\Delta \rho\|_F > \varepsilon$ 
     $\rho^{n+1} = (\hat{C} \hat{C}^T + \lambda_r I)^{-1} (\hat{C} G^T + \lambda_r (r^n - b_r^n))$ ,

```

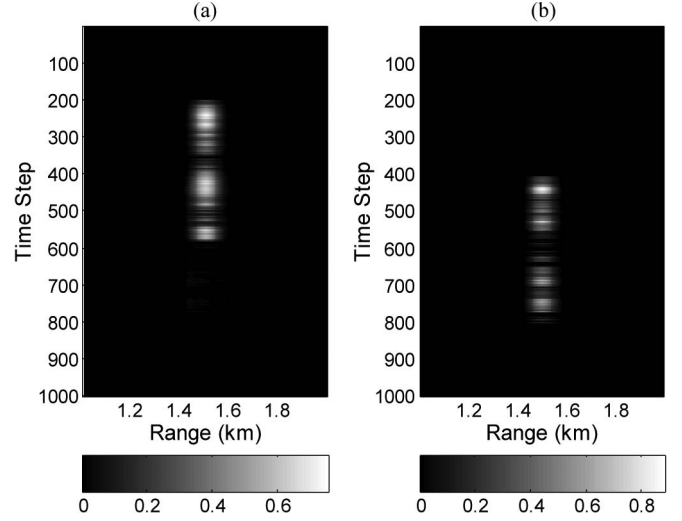


Fig. 3. Concentration estimates from simulated data. (a) Bioaerosol. (b) Interferent.

$$\begin{aligned} r^{n+1} &= (\rho^{n+1} + b_r^n - \mu_\rho / \lambda_r)^+ / \\ &\quad \|(\rho^{n+1} + b_r^n - \mu_\rho / \lambda_r)^+\| \\ b_r^{n+1} &= b_r^n + \rho^{n+1} - r^{n+1}, \\ \Delta \rho &= \rho^{n+1} - \rho^n, \\ n &\rightarrow n + 1, \end{aligned}$$

end

$$\hat{\rho} = \rho^{n+1}, D\rho = \|\hat{\rho} - \rho_{\text{old}}\|_F, \rho_{\text{old}} = \hat{\rho}$$

end

Output $\hat{\rho}$ and \hat{C}

V. NUMERICAL EXAMPLES

In this section, we illustrate the multi-aerosol unmixing algorithm on simulated and actual release data collected by the U.S. Army Frequency Agile Lidar (FAL) sensor. The calculations were done by implementing Algorithm 2 in MATLAB on a PC. The simulated FAL data were created by injecting two overlapping aerosol plumes having Gaussian range dependence both centered at 1.5 km with width 50 m into background FAL data sets. Those sets consisted of transmitted pulse waveforms and received laser backscatter from the natural atmosphere as a function of time step, wavelength index, and range cell. The two injected plumes represent a bioaerosol simulant (bacillus BG) and interferent (kaolin dust). The simulant plume was injected between time steps 200 and 600, and the interferent between time steps 400 and 800. A randomly varying peak concentration was created from a first-order AR model. The purpose of the simulator was to generate data for overall algorithm performance verification including background removal and transmitter pulse deconvolution. Because those operations are not relevant to the present discussion, we focus on the comparison of the input concentration and backscatter waveforms with the estimates from the split Bregman algorithm after data preprocessing.

Fig. 3 shows the concentration estimates from the unmixing algorithm with regularization parameters set at $\lambda_r = \lambda_c = 0.05$

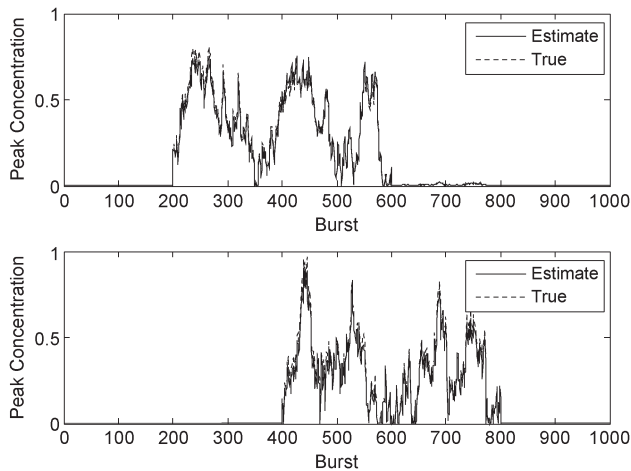


Fig. 4. Split Bregman peak concentration estimates from simulated data. (Top) Bioaerosol. (Bottom) Interferent.

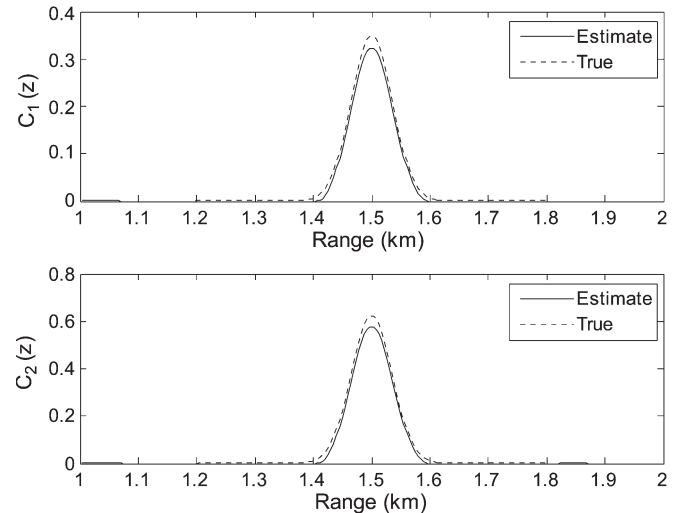


Fig. 6. Concentration range dependence from simulated data. (Top) Bioaerosol. (Bottom) Interferent.

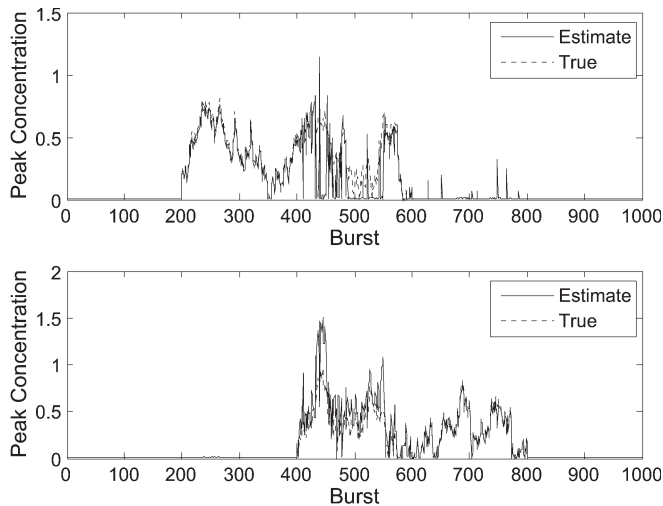


Fig. 5. Bayes processor peak concentration estimates from simulated data. (Top) Bioaerosol. (Bottom) Interferent.

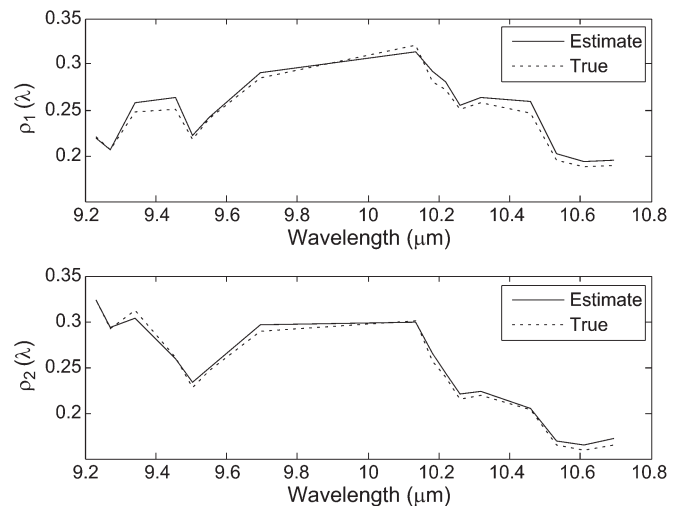


Fig. 7. Backscatter wavelength dependence from simulated data. (Top) Bioaerosol. (Bottom) Interferent.

and $\mu_\rho = \mu_C = \lambda_r^2$. The plots show the bioaerosol estimates (left) and interferent (right) versus time step and range. The calculation was initialized using the mean of the backscatter spectral estimates used to train our SVM classifier for the bioaerosol and interferent classes.

Fig. 4 compares the input and estimated peak concentration over range as a function of time step for the bioaerosol (top) and interferent (bottom). We see that the estimates track the input throughout the run including the plume overlap region. For comparison, Fig. 5 plots the peak concentration estimates from a previous algorithm based on using backscatter mean spectra as priors in a Bayesian scheme. Since the prior as well as data densities were chosen to be Gaussian, the Bayes approach in effect is doing quadratic norm processing. Although giving good results when the plumes are separated in time, this processor fails to produce good material separation in the overlap region.

Figs. 6 and 7 compare the concentration range dependence (true and estimated) and backscatter wavelength dependence

at time steps 300 and 700 for the bioaerosol and interferent, respectively. The results suggest that the split Bregman unmixing can provide both low bias and low variance estimates.

As an example of processing FAL data from a mixture of aerosols, we consider the partially overlapped release TD4065 of Florida BG (a bioaerosol simulant) and Kuwait dust on May 31, 2008 in the Joint Ambient Breeze Tunnel (JABT) at Dugway Proving Ground, UT. The FAL sensor was located about 1.2 km from the entrance to the JABT. The bioaerosol was released between time steps 100 and 476, and the dust between times 261 and 633. Data collected during the first 100 time steps were used to estimate the backscatter from the natural atmosphere. The aerosols were injected near the far end of the tunnel and drawn toward the front of the tunnel by large fans, where they were exhausted.

Fig. 8 shows the concentration estimates from the unmixing algorithm on these data with the bioaerosol (dust) plotted on the left (right). We see the initial localized aerosol appearing at

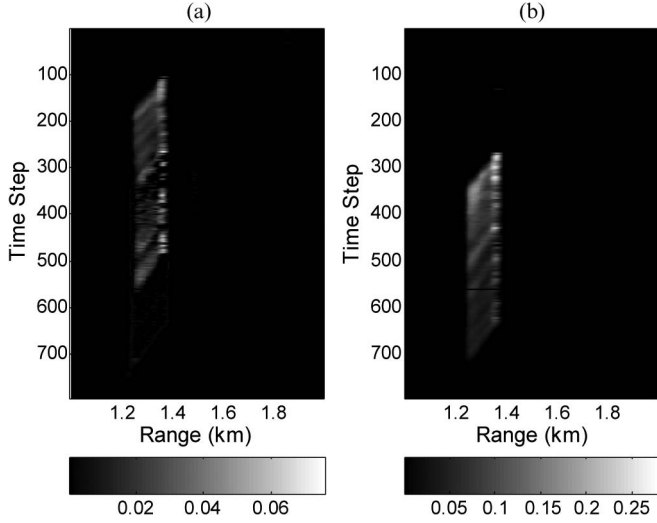


Fig. 8. Concentration estimates from JABT release. (a) Bioaerosol. (b) Interferent.

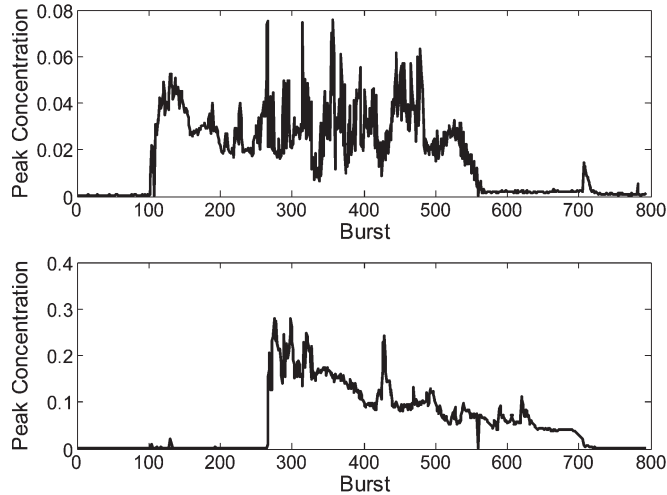


Fig. 9. Peak concentration estimates from JABT release. (Top) Bioaerosol. (Bottom) Interferent.

the indicated beginning of the releases. The subsequent time steps show the plumes expanding to fill the space between the injection and extraction locations. Fig. 9 plots the peak concentration over range with the bioaerosol (dust) shown at the top (bottom). We see a clean separation of the two aerosol components in these figures.

The estimates of aerosol backscatter are plotted in Fig. 10 as a function of time step and wavelength index for the 16 wavelengths used in these tests. Up to time step 100, we see only the random unit vectors produced by the algorithm in the absence of concentration. After the bioaerosol release (shown on the left), the estimates display a consistent structure, although they are rather noisy between time steps 300 and 450 because of low concentration levels. The corresponding dust backscatter estimates (shown on the right) also indicate a consistent structure throughout the dust release.

Finally, the aerosol classifier, a least-squares SVM classifier [10], was applied to the backscatter estimates. Our classifier

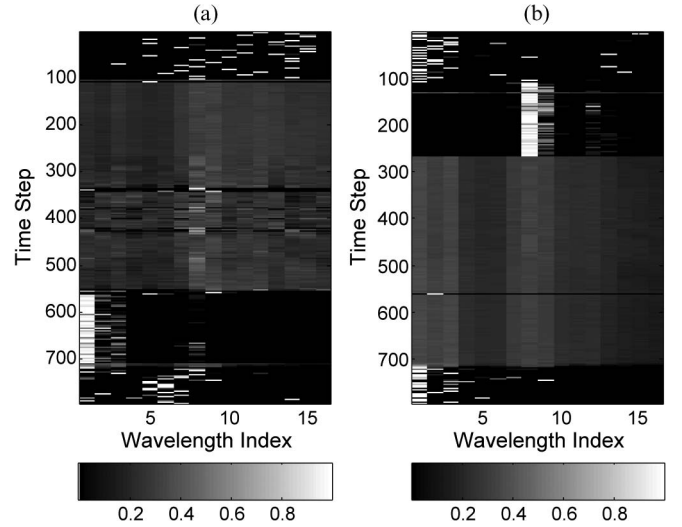


Fig. 10. Backscatter estimates from JABT release. (a) Bioaerosol. (b) Interferent.

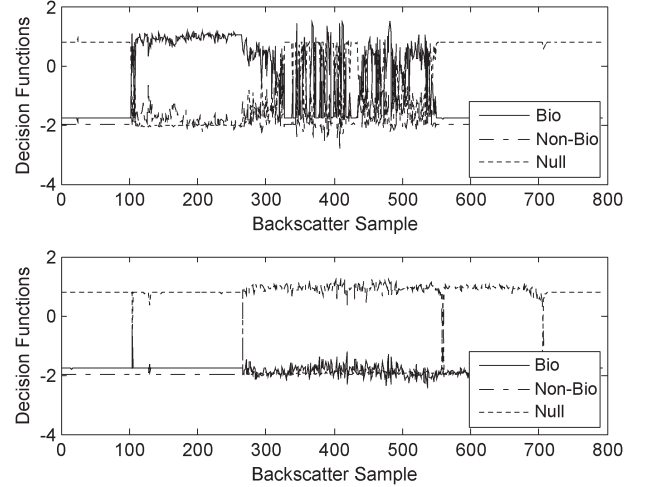


Fig. 11. Classifier decision functions from JABT release. (Top) Bioaerosol. (Bottom) Interferent.

consists of a three-class discriminator for bioaerosol, interferent, and null classes. The latter class was included to allow the classifier to perform a detection function by rejecting spectral patterns that look like neither bioaerosol nor interferent. Three binary classifiers were trained by the 1-versus-rest method for discriminating samples from each class against the pooled alternatives. At each time step, the class whose classifier has the highest decision function value is chosen. Backscatter estimates from both material components were processed this way, and the results for the decision functions are plotted in Fig. 11. The results indicate that the classifier recognized both materials at the correct times during the partially overlapped releases.

VI. SUMMARY AND CONCLUSION

The unmixing of elastic backscatter data from multi-wavelength, range-resolved lidar for aerosol mixtures has defied solution by traditional regularization methods using

quadratic smoothing constraints. A new shrinkage-based L_1 -regularization method for linear inverse problems, the split Bregman algorithm, has been successfully applied to the aerosol unmixing problem. It was illustrated here on simulated and actual aerosol mixture release data collected by U.S. Army personnel in field testing at Dugway proving Ground, UT using the rapidly tuned FAL sensor.

The capability of resolving data from mixtures of aerosols into their backscatter and concentration components is important to the success of standoff sensors for biological detection in realistic operating environments where interferent materials such as smoke and dust will usually be present. Failure to correctly perform this unmixing can lead to increased misclassifications that degrade the usefulness of potential sensors employing active detection.

Other possible standoff sensing applications of this unmixing technique include: 1) the analysis of lidar data from chemical releases where the agent can have both vapor and aerosol phases and interferent materials can include byproducts of an explosive release, and 2) the use of thermal imaging sensors operating in the long wave IR spectra region.

APPENDIX AUGMENTED LAGRANGIAN DERIVATION OF SPLIT BREGMAN

Given the augmented Lagrangian function $L(u, d, b)$ in (12), we wish to find a saddle point (u^*, d^*, b^*) such that¹

$$L(u^*, d^*, b) \leq L(u^*, d^*, b^*) \leq L(u, d, b^*). \quad (23)$$

We solve this saddle point problem by iterating between primal and dual optimizations

$$\begin{aligned} (u^{k+1}, d^{k+1}) &= \arg \min_{u, d} L(u, d, b^k) \quad (\text{primal}) \\ b^{k+1} &= b^k + u^{k+1} - d^{k+1} \quad (\text{dual}). \end{aligned} \quad (24)$$

For the primal minimizations holding the dual variable b fixed, we note that because of the introduction of the d variables, the optimization over u can be done for fixed d by differentiation

$$\frac{\partial L(u, d, b)}{\partial u} = K^T(Ku - f) + \lambda b + \lambda(u - d) \quad (25)$$

to get

$$u^{k+1} = (K^T K + \lambda I)^{-1} (K^T f + \lambda(d^k - b^k)). \quad (26)$$

Likewise, although the d variable optimization is still non-smooth, it is very easy to solve by shrinkage for given u and b

$$d^{k+1} = S_{\mu/\lambda}(u^{k+1} + b^k) \quad (27)$$

¹This sketch follows the split Bregman treatment given by Gui-Bo and Xiaohui [6].

where the shrinkage function S_λ is given by (13). Steps (26) and (27) can be iterated for fixed b^k , but we find it more efficient (usually) to perform them only once.

ACKNOWLEDGMENT

The authors wish to acknowledge the substantial improvements made to the paper by the reviewers.

REFERENCES

- [1] R. E. Warren, R. G. Vanderbeek, A. Ben-David, and J. L. Ahl, "Simultaneous estimation of aerosol cloud concentration and spectral backscatter from multiple-wavelength lidar data," *Appl. Opt.*, vol. 47, no. 24, pp. 4309–4320, Aug. 2008.
- [2] The text *Elastic Lidar*, by V. Kovalev and W. Eichinger (Wiley 2004) has an extensive treatment of lidar analysis methods for continuously distributed aerosols and a bibliography of over 700 references.
- [3] T. Goldstein and S. Osher, "The split Bregman method for L_1 -regularized problems," *SIAM J. Imag. Sci.*, vol. 2, no. 2, pp. 323–343, Feb. 2009.
- [4] W. Yin, S. Osher, D. Goldfarb, and J. Darbon, "Bregman iterative algorithms for l_1 -minimization with application to compressed sensing," *SIAM J. Imag. Sci.*, vol. 1, no. 1, pp. 143–168, 2008.
- [5] X. Tai and C. Wu, "Augmented Lagrangian method, dual methods and split Bregman iteration for ROF model," in *Scale Space and Variational Methods in Computer Vision: Lecture Notes in Computer Science*, vol. 5567. Berlin, Germany: Springer-Verlag, 2009, pp. 502–513.
- [6] Y. Gui-Bo and X. Xiaohui, "Split Bregman for large scale fused Lasso," *J. Comput. Stat. Data Anal.*, vol. 55, no. 4, pp. 1552–1569, Apr. 2011.
- [7] E. Esser, "Applications of Lagrangian-based alternating direction methods and connections to split Bregman," Univ. California, Los Angeles, CA, UCLA CAM Rep. 09-31, 2009.
- [8] N. Keshava, J. Kerekes, D. Manolakis, and G. Shaw, "An algorithm taxonomy for hyperspectral unmixing," in *Proc. SPIE—Algorithms Multispectral, Hyperspectral, Ultraspectral Imagery VI*, S. Shen and M. Descour, Eds., 2000, vol. 4049.
- [9] S. Boyd and L. Vandenberghe, *Convex Optimization*. Cambridge, U.K.: Cambridge Univ. Press, 2004.
- [10] J. A. K. Suykens, T. Van Gestel, J. De Brabanter, B. De Moor, and J. Vandwalle, *Least Squares Support Vector Machines*. Singapore: World Scientific, 2002.



Russell E. Warren (M'88) received the Ph.D. degree in physics from the University of Iowa, Iowa City.

He is president of EO-Stat Inc., a privately held company specializing in statistical signal processing and machine learning applied to data from electro-optical sensors. Prior to founding EO-Stat, he was a Principal Scientist at SRI International. Current interests include developing classifiers based on the support vector machine for standoff sensing of bioaerosols, and inferring the spectral and concentration properties of chemical and biological materials in the atmosphere from multiwavelength rapidly tuned lidar data.



Stanley J. Osher received the Ph.D. degree in mathematics from New York University's Courant Institute of Mathematical Sciences.

He is currently a Professor of mathematics, computer science and engineering at the University of California, Los Angeles (UCLA). He is also an Associate Director of the National Science Foundation-funded Institute for Pure and Applied Mathematics. He is a member of the National Academy of Sciences, the American Academy of Arts and Sciences, and is one of the top 25 most highly cited

researchers in both mathematics and computer sciences. He has received numerous academic honors and has cofounded three successful companies, each based largely on his own (joint) research. His current interests mainly involve information science which includes graphics, image processing, compressed sensing, and machine learning. He has co-invented and/or codeveloped the following widely used algorithms: 1) essentially non-oscillatory (ENO), weighted ENO and other shock capturing schemes for hyperbolic systems of conservation laws and their analogs for Hamilton-Jacobi equations; 2) the level set method for capturing dynamic surface evolution; 3) total variation and other partial differential-based methods for image processing; 4) Bregman iterative methods for L1 and related regularized problems which arise in compressive sensing, matrix completion, imaging, and elsewhere; 5) diffusion generated motion by mean curvature and other threshold dynamic methods.



Richard G. Vanderbeek received the B.S. degree in electrical engineering from Drexel University, Philadelphia, PA, and the M.S. degree in electrical engineering from Johns Hopkins University, Baltimore, MD.

He is the Branch Chief for Laser Standoff Detection at the Edgewood Chemical Biological Center. He has been active in the development of Laser Standoff Detection systems for 17 years and most recently been the Principal Investigator for the development of the next-generation biological standoff

detection technologies.